

Study of primary circulation loop and flow macro-formation dynamics in a baffled mixing vessel with an axial impeller

Tomáš Brůha^a *, Milan Jahoda^a ., Ivan Fořt^b ., Oldřich Brůha^b .

^a) Department of Chemical Engineering, Institute of Chemical Technology, Prague
Technická 5, 166 28 Praha 6, Czech Republic

^b) Department of Process Engineering, Faculty of Mechanical Engineering Czech
Technical University, Technická 4, 166 07 Praha 6, Czech Republic

enex@volny.cz

The paper deals with experimental and theoretical study of flow pattern dynamics in a flat-bottomed cylindrical stirred tank of inner diameter $T = 0.29$ m, filled with water to the height $H = T$. The vessel was equipped with four radial baffles and stirred with six pitched (45°) blade impeller with impeller speed 400 rpm. The flow was observed in vertical and horizontal planes passing through the vessel. Visualized flow patterns of agitated liquid were recorded and analyzed with respect to characteristics and dynamics of flow macro-formations. Experimental results were compared with results coming from proposed a theoretical model of flow macro-formations.

1. Introduction

This study follows our previous investigation of the flow macro-formations (FMF) and primary circulation loop behaviour/oscillation (Brůha et al., 2007). Some of characteristics of this investigated behaviour are considered to be in a strong correlation with the occurrence of flow macro-instabilities (FMIs), a phenomenon which has been studied and described by several authors (Brůha et al., 1996; Hasal et al., 2000; Paglianti et al., 2006; Roussinova et al., 2003). The main object of this study is experimental and theoretical analysis of appearance and dynamics of flow macro-formation, which is periodically generated by the primary circulation loop (PCL) and after separating, moving vertically upwards to the liquid surface and finally disintegrating (Brůha et al., 2007; Brůha et al., 2008). Such flow-macro formations (FMF) are supposed to be a manifestation of FMIs in the investigated cylindrical system with axial flow impeller and radial baffles.

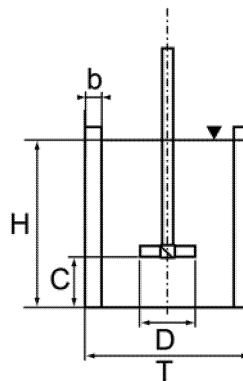


Figure 1. Scheme of vessel

2. Experimental

The experiments were done in a flat-bottomed cylindrical stirred tank of inner diameter $T = 0.29$ m, filled with water to the height $H = T$, see Fig.1. The vessel was equipped with four radial baffles, (width of baffles $b = 0.1T$) and stirred with six pitched blade impeller (pitch angle 45° , impeller diameter $D = T/3$, width of blade $u = D/5$), pumping downwards. Flow patterns of agitated liquid were visualized by means of aluminum micro particles spread in water and illuminated by a vertical light knife 5 mm wide. The impeller speed was 400 rpm (turbulent flow regime, $Re_M = 6.22 \cdot 10^4$) and the impeller off bottom clearance was $T/3$. The flow was observed both in a vertical plane passing through the vessel (vertical section of the vessel) in front of the adjacent baffles and in three horizontal planes with heights above vessel bottom of 0.18, 0.25 and 0.285 m.

3. Methods

The visualised flow was recorded repeatedly in 25 seconds time intervals in the vertical plane and in 10 seconds time intervals in all the three above defined levels of the horizontal plane. Each of the records was resolved into short time interval shots and the acquired series of shots were analyzed by an appropriate graphic software. The total number of shots for respective planes ranged from 250 to 1200.

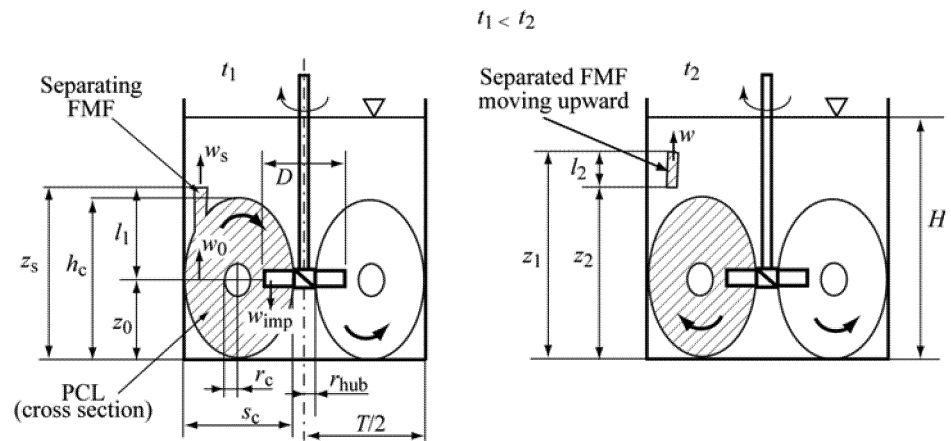


Figure 2. Scheme of PCL in mixing vessel with generated and separated FMF

The characteristics observed and analyzed from vertical plane visualisation were: *size* of the PCL vertical section and size of its core; *height*, h_c , and *width*, s_c , of PCL in the moment of the FMF origination; *equivalent* diameter of PCL core, r_c , (see Fig. 2); *time* of the FMF generating, t_g , and *time* of its separation from the PCL, t_s ; its *positions* z_g and z_s (see Figs. 3 and 4); *upper* off-bottom clearance z_1 and *lower* off-bottom clearance z_2 of separated FMF; *time* of the FMF disintegration, t_d , below surface level and its *position*, z_d , see Fig. 4.

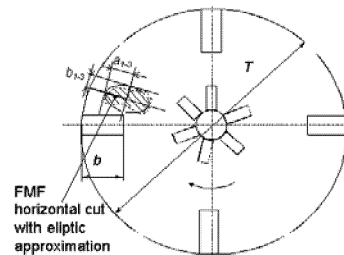


Figure 3. Horizontal visualisation

The characteristics observed and analyzed from horizontal planes visualisation were: *size* and position of the FMF horizontal projection and axes a_{1-3} , b_{1-3} of elliptically approximated horizontal projection of FMF, see Fig. 3.

Values calculated from the data obtained: area A_c of the PCL mean peripheral projection in a horizontal plane at the moment of the flow macro-formation generation. The shape of PCL was considered as a toroid with an elliptical projection in the mixing vessel r - z plane (Brůha et al., 2007), assuming that the PCL fills up a half width of active impeller area, where r_{imp} is radius of impeller hub, see Fig. 2.

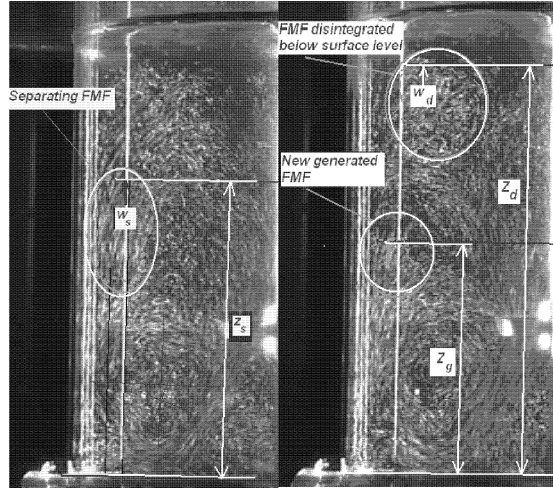


Figure 4. Visualization of separating and disintegrating FMF

$$A_c = \pi \left[\left(s_c + \frac{r_{hub}}{2} + \frac{D}{4} \right)^2 - \left(\frac{s_c + r_{hub} + r_c}{2} + \frac{D}{4} \right)^2 \right] \quad (1)$$

Mean axial flow velocity through area A_c (according to the equation of continuity) is

$$w_0 A_c = w_{imp} A_{imp} \Rightarrow w_0 = w_{imp} \frac{A_{imp}}{A_c}, \quad \text{where } A_{imp} = \pi \left(\frac{D^2}{4} - r_{hub}^2 \right) \quad (2)$$

is the discharge area of rotating impeller, and w_{imp} is impeller discharge velocity with value calculated from impeller pumping number $w_{imp} = 0.863 \text{ ms}^{-1}$ (Brůha et al., 2007).

Based on values w_0 , dimensionless axial velocity gradient, VG , was calculated (Bittorf et al., 2000):

$$VG = \frac{w_0}{V_{tip}} \frac{T}{r} = \frac{w_0}{\pi n D} \frac{T}{\left(s_c + \frac{r_{hub}}{2} + \frac{D}{4} \right)} \quad (3)$$

Next experimental characteristics were obtained:

equivalent diameter for elliptically approximated area of horizontal cross section of flow macro-formation (see Fig. 3), $d_{1-3} = (4 a_{1-3} b_{1-3})^{0.5}$; mean vertical size of generated flow macro-formation before separation (see Fig. 2), $l_1 = 0.5 (z_g + z_s - h_c)$; vertical size of separated FMF, $l_2 = z_1 - z_2$; total path length of generated FMF before separation, $s_1 = z_s - z_g$; total path length of separated FMF, $s_2 = z_d - z_s$; experimental time of FMF rising before separation, $t_{1exp} = t_s - t_g$; experimental time of movement separated FMF before disintegration, $t_{2exp} = t_d - t_s$; total experimental time of FMF existence, $t_{Cexp} = t_{1exp} - t_{2exp}$. Average calculated values of equivalent diameter d_{1-3} for measured values of $C_{1-3} = 0.18; 0.25; 0.285$ m were 56.4, 53.7 and 51.2 mm, respectively. Linear dependence of d on C (or z coordinate) was obtained by regression, $d = -0.047z + 65$.

4. Theoretical

Theoretical analysis of flow macro-formation dynamics begins from equation expressing the balance of forces acting on FMF and describing a corresponding motion equation. For this purpose, the FMF is considered to be an object moving in a medium of defined viscosity. Densities of the medium and of the macro-formation are identical.

Simplifying assumptions of our solution are follows:

- FMF is cylinder with sizes d , l , swelling base and moving in direction of its axis,
- the shape and vertical size l of FMF remain constant during movement,
- the initial axial velocity of FMF is equal to the velocity in the position of FMFs origin inside the PCL.

Equation of force balance:

$$m \, dw / dt + F_h - F_r - G = 0, \quad (4)$$

contains the hydrostatic, resistance and gravity forces:

$$F_h = V_{FMF} \rho g, \quad F_r = 0.5 C_x A_{FMF} \rho w^2, \quad G = V_{FMF} \rho g, \quad (5)$$

where V_{FMF} is volume of flow macro-formation, A_{FMF} – frontal area of flow macro-formation and ρ – liquid density. According to Eq. (4) we get

$$\rho V_{FMF} \, dw / dt + V_{FMF} \rho g - 0.5 C_x A_{FMF} \rho w^2 - V_{FMF} \rho g = 0 \quad . \quad (6)$$

After treatment, we obtain

$$\int_{w_0}^w \frac{dw}{w^2} = - \frac{C_x A_{FMF} \rho}{2 A_{FMF} l \rho} \int_0^t dt \Rightarrow s = \int_0^t w(t) dt \Rightarrow w(s) = w_0 \exp[-C_x s / (2l)] \quad . \quad (7)$$

Finally solution is

$$t = [\exp(-C_x s / (2l)) - 1] l / (C_x w_0) \quad . \quad (8)$$

For determination of values of resistance coefficient C_{x1} and C_{x2} , value of C_x for cylinder moving in direction of its axis (depends on l/d) obtained from literature was averaged with C_x for semi sphere (0.3-0.4) (Buckwalter et al., 1987), because of the swelling base of cylinder. Mean axial positions of FMF were determined as $z_{m1} = (z_s + z_g)/2$ and $z_{m2} = (z_d + z_s)/2$. During the first step of solution of Eqs. (7 and 8), we obtained the axial velocity and rising time of FMF at the moment of its separation:

$$w_s = w_0 \exp[-C_{x1} s_1 / (2l_1)], \quad t_1 = [\exp(-C_{x1} s_1 / (2l_1)) - 1] l_1 / (C_{x1} w_0) \quad . \quad (9)$$

During the second step, we obtained the final axial velocity of FMF (velocity at the disintegration) and the time of movement of the separated FMF:

$$w_d = w_s \exp[-C_{x_2} s_2 / (2l_2)], t_2 = [\exp(-C_{x_2} s_2 / (2l_2)) - 1] l_2 / (C_{x_2} w_s) \quad (10)$$

Finally, total time of flow macro-formation existence holds $t_c = t_1 + t_2$.

5. Results

Total number of analyzed flow macro-formation realizations in 25 s long record was 22 and experimental and calculated values of total time of FMF existence are presented in Table 1. Average relative difference between experimental and calculated total times of FMF existence (from Table 1.) is 15.9 %. This model does not solve interaction of flow macro-formation with water level (surface tension forces are not included) and thus flow macro-formations which reached almost surface level ($z_d/H > 0.9$) were excluded from the FMF analyse. The horizontal visualisation confirmed previous finding of incidence of flow macro-formation and strong axial current purely at the baffles, while area of horizontal cross-section of FMF slightly decreases with off-bottom clearance increasing.

Table 1: Experimental and theoretical times of FMF existence

z_B (m)	0.109	0.118	0.124	0.135	0.139	0.142	0.145	0.146	0.150	0.150	0.151
t_c (s)	0.755	0.814	0.525	0.58	0.825	0.38	0.39	0.527	0.429	0.849	0.368
$t_{c, \text{exp}}$ (s)	0.745	1.07	0.599	0.5	0.632	0.41	0.35	0.53	0.375	0.928	0.309
z_B (m)	0.153	0.153	0.154	0.169	0.171	0.172	0.185	0.186	0.191	0.194	0.211
t_c (s)	0.514	0.518	0.313	0.42	0.306	0.27	0.18	0.442	0.245	0.319	0.186
$t_{c, \text{exp}}$ (s)	0.48	0.566	0.363	0.52	0.207	0.21	0.15	0.333	0.18	0.345	0.231

Values of VG (Eq. 3) depending on $z_0/T (\cong h_c / 2T)$, see Fig. 2) are presented in Fig. 5.

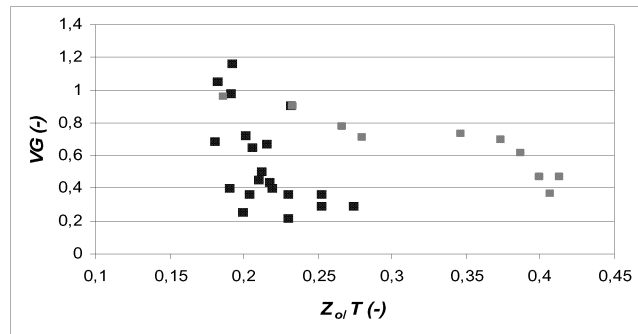


Figure 5. Effect of off-bottom clearance on VG : ■calculated data, □experimental data

6. Conclusions

Total time of FMF existence can be considered as confirmation of theoretical model correctness, with respect to introduced simplifying assumptions and relatively low accuracy of time measurement due to dispersion of generated time steps (0.025 - 0.04 s). Founded values of z_s show that separation of FMF from PCL takes place within interval $z_s/H = 0.55 - 0.75$ i.e. around height of active volume of mean circulation as previously

reported Bittorf et al. (2000). The effect of off-bottom clearance on calculated dimensionless velocity gradient (Fig. 5.) is in a good agreement with previous experimental result for the same system and conditions with respect to usage four 45° pitched blade impeller (Bittorf and Kresta, 2000). Values of the initial axial position z_g of the FMF generating are within limits 0.109 - 0.211 m and generally take place around coordinate $H/2$. Values of axial position z_d of FMF disintegration are within limits 0.226 - 0.260 m, it means that it takes place at positions $>0.78 H$. Axial velocity of FMF near disintegration w_d is within limits 0.063 - 0.245 ms^{-1} and therefore takes place between 0.073 - 0.284 w_{imp} . Values of FMF path length s_1 and s_2 are within limits 0.010 - 0.107 m and 0.015 - 0.108 m e.g. in very similar intervals. Values of vertical size of FMF l_1 and l_2 are within limits 0.005 - 0.141 and 0.012 - 0.078, so value of l_1 shows a markedly higher dispersion than value l_2 . Analysis of correlations showed that there is no significant correlation among values z_s , z_g , z_d and s_1 , s_2 resp. l_1 , l_2 .

Acknowledgements

Authors are grateful to the Czech Ministry of Education (MSM 6046137306) and to the Czech Science Foundation (104/09/1290) for providing research support.

References

- Bittorf K.V., Kresta, S.M., 2000, Active Volume of Mean Circulation for Stirred Tanks Agitated with Axial Impellers. *Chemical Engineering Science* 55, 1325-1335
- Brůha, O., Fořt I., Smolka P., Jahoda M., 1996, Experimental Study of Turbulent Macroinstabilities in an Agitated System with Axial High-speed Impeller and Radial Baffles, *Collection of Czechoslovak Chemical Communications* 61, 856-867
- Brůha O., Brůha T., Fořt I., Jahoda M., 2007, Dynamics of the Flow Pattern in a Baffled Mixing Vessel with an Axial Impeller, *Acta Polytechnica* 47/6, 17-26
- Brůha T., Jahoda M., Fořt I., Brůha O., 2008, Impact of Primary Circulation Loop Oscillation on Flow Macro-Instability in a Baffled Mixing Vessel with an Axial Impeller, 35th Conference SSCHE, Tatranske Matliare, Slovakia, 252
- Buckwalter G.L. and Riban D.M., 1987, *College Physics*, McGraw Hill Book Comp
- Hasal P., Montes J-L., Boisson H.C., Fořt I., 2000, Macro-instabilities of Velocity Field in Stirred Vessel, Detection and Analysis, *Chemical Engineering Science* 55, 391-401
- Kresta S.M., Wood P.E, 1993, The Mean Flow Field Produced by a 45° Pitched Blade Turbine: Changes in the Circulation pattern Due to Off Bottom Clearance, *The Canadian Journal of Chemical Engineering* 71, 52-42
- Paglianti A., Montante G., Magelli F., 2006, Novel Experiments and Mechanistic Model for Macroinstabilities in Stirred Tanks, *AIChE Journal* 52, 426-437
- Roussinova V.T., Kresta S.M., Weetman R., 2003, Low Frequency Macroinstabilities in Stirred Tank: Scale-up and Prediction Based on Large Eddy Simulations, *Chemical Engineering Science* 58, 2297-2311